Measurements and Thermodynamic Modeling of Vapor−Liquid Equilibria in Ethane−Water Systems from 274.26 to 343.08 K

ARTICLE *in* INDUSTRIAL & ENGINEERING CHEMISTRY RESEARCH · JUNE 2004

Impact Factor: 2.59 · DOI: 10.1021/ie049747e

4 AUTHORS:

Amir H. Mohammadi

552 PUBLICATIONS **4,825** CITATIONS

SEE PROFILE

Antonin Chapoy

Heriot-Watt University

106 PUBLICATIONS **1,669** CITATIONS

SEE PROFILE

Bahman Tohidi

Heriot-Watt University

216 PUBLICATIONS **3,099** CITATIONS

SEE PROFILE

Dominique Richon

Aalto University

533 PUBLICATIONS **6,603** CITATIONS

SEE PROFILE

Measurements and Thermodynamic Modeling of Vapor−Liquid Equilibria in Ethane−Water Systems from 274.26 to 343.08 K

Amir H. Mohammadi,[†] Antonin Chapoy,[‡] Bahman Tohidi,[†] and Dominique Richon*[,‡]

Centre for Gas Hydrate Research, Institute of Petroleum Engineering, Heriot-Watt University, Edinburgh EH14 4AS, Scotland, U.K., and Centre d'Energétique, Ecole Nationale Supérieure des Mines de Paris (CENERG/TEP), 35 rue Saint Honoré, 77305 Fontainebleau, France

In this paper, new experimental data on the solubility of gaseous ethane in water are reported in the 274.26−343.08 K temperature range for pressures up to 4.952 MPa. A static−analytic apparatus, taking advantage of a pneumatic capillary sampler, is used for fluid sampling. The Valderrama modification of the Patel−Teja equation of state, combined with non-density-dependent mixing rules, is used for modeling the vapor−liquid equilibrium. The new solubility data generated in this work are used for tuning of the binary interaction parameters between ethane and water. Then, these data are compared with some literature data and the results of the thermodynamic model. To further evaluate the performance of the model, a comparison is made between the predicted water content data and some experimental data in the literature. These comparisons show the reliability of the techniques and model presented in this work.

1. Introduction

Accurate information on the phase behavior of natural gas components and water is crucial to the design and optimization of operating conditions of natural gas facilities and to the avoidance of condensate, ice, and gas hydrate formation during production, transportation, and processing of natural gases. On the other hand, hydrocarbon solubility in water is an important issue from an environmental aspect, because of new legislations and restrictions on the hydrocarbon content in water disposal.

Therefore, it is of great interest to study the phase equilibrium in a water−hydrocarbon system. Accurate solubility data, especially at low-temperature conditions, are necessary to develop and verify thermodynamic models. However, preliminary studies show that most of the experimental data for hydrocarbons and for non-hydrocarbon gases (e.g., N_2, CO_2, and H_2S) have been reported at relatively high temperatures, and the data reported at low temperatures are often inconsistent with very large uncertainties that may lead to huge deviations for predictive methods.[1,2]

Only a few studies have been reported on the solubility of ethane in water. This is partly due to the low solubility of ethane in water because the solubility of hydrocarbons decreases with the number of carbon atoms. Tables 1 and 2 give a list of some data on the ethane solubility in water and the water content of ethane at different conditions, respectively.

In this work, new solubility measurements of gaseous ethane in water have been generated in a wide temperature range, i.e., 274.26−343.08 K and pressures up to 4.952 MPa. The different isotherms presented herein were obtained using an apparatus based on a static−analytic method, taking advantage of a capillary sampler.[1,2,11,24−26]

Table 1. Experimental Solubility of Ethane in Water at Pressures over Atmospheric Pressure

reference	*T*/K	*P*/MPa
Wang et al.[3]	283.2−303.2	0.5−4
Kim et al.[4]	298.15	1.4−3.9
Reichl[5]	283.17−343.16	0.188−0.267
Danneil et al.[6]	473.15−673.15	20−370
Anthony and McKetta[7]	344.26−377.65	3.479−28.162
Czerski and Czaplinski[8]	273.15	0.1013−0.5066
Culberson and McKetta[9]	310.93−444.26	0.407−68.481
Culberson et al.[10]	310.93−444.26	0.407−8.375

The Valderrama modification of the Patel−Teja equation of state (VPT-EoS) [27] with non-density-dependent (NDD) mixing rules[28] is used to model the vapor−liquid equilibrium. The binary interaction parameters (BIPs) between ethane and water are tuned using the new experimental results on gaseous ethane solubility data. Then, the new experimental data and some literature data are compared with the results of the model. To further evaluate the performance of the model, some independent water content data in the literature are compared with the predictions of the model. Predictions are found to be in good agreement with the experimental data, demonstrating the reliability of the experimental technique and the model used in this work.

2. Experimental Section

2.1. Materials. Ethane was purchased from Messer Griesheim with a certified purity of greater than 99.995 vol %. Helium from Air Liquide is pure grade with traces of water (3 ppm) and of hydrocarbons (0.5 ppm). Osmosed water was used after degassing.

2.2. Apparatus and Experimental Procedures. The apparatus used in this work (Figure 1) is based on a static−analytic method with fluid-phase sampling. This apparatus is similar to that described by Laugier and Richon.[29]

The phase equilibrium is achieved in a cylindrical cell made of sapphire, the cell volume is about 28 cm^3 (internal diameter = 25 mm), and it can be operated up to 8 MPa between 223.15 and 473.15 K. The cell is immersed in an Ultra-Kryomat Lauda constant-tem-

* To whom correspondence should be addressed. Tel.: +(33) 1 64 69 49 65. Fax: +(33) 1 64 69 49 68. E-mail: richon@paris.ensmp.fr.

[†] Heriot-Watt University.

[‡] Ecole Nationale Supérieure des Mines de Paris.

10.1021/ie049747e CCC: $27.50
Published on Web 07/01/2004

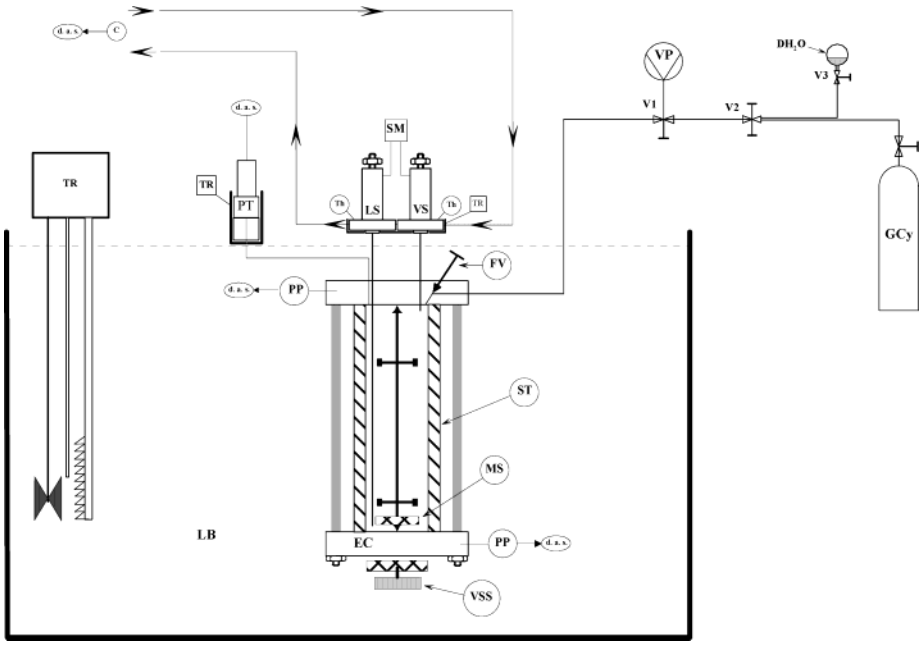

Figure 1. Flow diagram of the equipment:[1,2,11,24−26] C, carrier gas; d.a.s., data acquisition system; DH_2O, degassed water; EC, equilibrium cell; FV, feeding valve; GCy, gas cylinder; LB, liquid bath; LS, liquid sampler; PP, platinum resistance thermometer probe; PT, pressure transducer; SM, sampler monitoring; ST, sapphire tube; Th, thermocouple; TR, temperature regulator; Vi, valve I; VS, vapor sampler; VSS, variable-speed stirrer; VP, vacuum pump.

Table 2. Experimental Water Content of Ethane[1]

reference	T_{min}/K	T_{max}/K	P_{min}/MPa	P_{max}/MPa
Mohammadi et al.[1]	282.93	293.10	0.506	2.990
Chapoy et al.[11]	278.08	303.11	0.323	4.63
Althaus[12]	253.15	293.15	0.5	3
Song and Kobayashi[13]	240.05	304.85	2.483	4.825
Namiot[14]	344.25	377.55	2.53	70.93
Song and Kobayashi[15]	240.05	304.85	2.483	4.825
Sloan et al.[16]	259.1	270.5	3.45	3.45
Bourrie and Sloan[17]	271.37	271.37	3.4464	3.4464
Sparks and Sloan[18]	259.1	270.45	3.447	3.447
Parrish et al.[19]	243.15	303.15	slightly above P^{sat}	slightly above P^{sat}
Pollin et al.[20] (Internal Report)	NA[a]	NA	NA	NA
Coan and King[21]	298.15	373.15	2.2798	3.6376
Anthony and McKetta[7]	310.93	410.87	2.5648	10.7956
Anthony and McKetta[22]	310.87	377.71	3.4237	34.655
Reamer et al.[23]	310.93	510.93	2.2112	68.2138

[a] NA = not available.

perature liquid bath that controls and maintains the desired temperature within ±0.01 K. To perform accurate temperature measurements in the equilibrium cell and to check for thermal gradients, the temperature is measured at two locations corresponding to the vapor and liquid phases through two 100 Ω platinum resistance thermometer devices [Pt(100)] connected to a Hewlett Packard data acquisition unit (HP34970A). These two Pt(100) devices are carefully and periodically calibrated against a 25 Ω reference platinum resistance thermometer (Tinsley Precision Instruments). The resulting uncertainty is not higher than ±0.04 K. The 25 Ω reference platinum resistance thermometer was calibrated by the Laboratoire National d'Essais (Paris) based on the 1990 International Temperature Scale (ITS 90). The pressure is measured by means of a Druck pressure transducer connected to the HP data acquisition unit (HP34970A); the pressure transducer is maintained at a constant temperature (temperature higher than the highest temperature of the study) by means of a specially made air thermostat, which is controlled using a proportional−integral−derivative regulator (West model 6100). The pressure transducer is calibrated against a dead weight pressure balance (Desgranges & Huot 5202S, CP 0.3−40 MPa, Aubervilliers, France). Pressure measurement uncertainties are estimated to be within ±1 kPa in the 0.2−6 MPa range.

The HP online data acquisition unit is connected to a personal computer through a RS-232 interface. This system allows real-time readings and storage of temperatures and pressures throughout the different isothermal runs.

The analytical work was carried out using a gas chromatograph (Varian model CP-3800) equipped with two detectors in series, a thermal conductivity detector (TCD) and a flame ionization detector (FID), connected to a data acquisition system (Borwin version 1.5, from JMBS, Le Fontanil, France). The analytical column is a Hayesep T 100/120 mesh column (silcosteel tube of length = 1.5 m and diameter = $^1/_8$ in.). The TCD was used to detect the water; it was repeatedly calibrated by injecting a known amount of water through liquid-tight syringes. The uncertainties on the calculated mole numbers of water are estimated to be within ±1.5% in the range of 2.5×10^{-5}−3×10^{-4} water mole number. The FID was used to detect the hydrocarbon. It was first

Table 3. Critical Properties and Acentric Factors[31]

compound	P_c/MPa	T_c/K	v_c/m^3·kmol^{-1}	ω
water	22.048	647.30	0.0560	0.3442
ethane	4.8798	305.42	0.1479	0.09896

calibrated by introducing known amounts of nitrogen through a gastight syringe; the mole number of nitrogen is thus known within ±1%. Following the nitrogen calibration, different gas mixtures of a known amount of nitrogen and of a small amount of ethane were prepared and loaded in the cell. Samples of different sizes were then withdrawn, and when the composition of the mixture is known and the mole number of nitrogen sampled is quantified, it is possible to estimate the amount of ethane and hence calibrate the FID. The resulting relative uncertainty is about ±0.9% in the mole number of ethane.

2.3. Experimental Procedures. The equilibrium cell and its loading lines were evacuated down to 0.1 Pa, and the necessary quantity of the preliminary degassed water (approximately 5 cm^3) was introduced using an auxiliary cell. Then, the desired amount of ethane was introduced into the cell directly from the commercial cylinder.

For each equilibrium condition, at least 10 samples of the liquid phase are withdrawn using the pneumatic sampler ROLSI[30] and analyzed in order to check for measurement repeatability. Because the volume of the withdrawn samples (less than 0.5−2 μg) is very small compared to the volume of the liquid phase present in the equilibrium cell (around 5 cm^3), it is possible to withdraw many samples without disturbing the phase equilibrium.

3. Thermodynamic Model

3.1. Pure Compound Properties. The critical temperature (T_c), critical pressure (P_c), critical volume (v_c), and acentric factor (ω) for each of the four pure compounds are provided in Table 3.

3.2. Model. A general phase equilibrium model based on the uniformity of the fugacity of each component throughout all of the phases[32,33] was used to model the vapor−liquid equilibria. The VPT-EoS[27] with the NDD mixing rules[28] was employed in calculating fugacities in fluid phases. This combination has proved to be a strong tool in modeling systems with polar as well as nonpolar components.[28]

The VPT-EoS[27] is given by

$$P = \frac{RT}{v-b} - \frac{a}{v(v+b)+c(v-b)} \tag{1}$$

with

$$a = \bar{a}\alpha(T_r) \tag{2}$$

$$\bar{a} = \frac{\Omega_a R^2 T_c^{\,2}}{P_c} \tag{3}$$

$$b = \frac{\Omega_b R T_c}{P_c} \tag{4}$$

$$c = \frac{\Omega_{c*} R T_c}{P_c} \tag{5}$$

$$\alpha(T_r) = [1 + F(1 - T_r^{\Psi})]^2 \tag{6}$$

where P is the pressure, T is the temperature, v is the molar volume, R is the universal gas constant, and $\Psi = 0.5$. The subscripts c and r denote critical and reduced properties, respectively.

The coefficients Ω_a, Ω_b, Ω_{c*}, and F are given by

$$\Omega_a = 0.66121 - 0.76105Z_c \tag{7}$$

$$\Omega_b = 0.02207 + 0.20868Z_c \tag{8}$$

$$\Omega_{c*} = 0.57765 - 1.87080Z_c \tag{9}$$

$$F = 0.46283 + 3.58230\omega Z_c + 8.19417(\omega Z_c)^2 \tag{10}$$

where Z_c is the critical compressibility factor and ω is the acentric factor. Tohidi-Kalorazi[34] relaxed the α function for water, α_w, using experimental water vapor pressure data in the range of 258.15−374.15 K, to improve the predicted water fugacity:

$$\alpha_w(T_r) = 2.4968 - 3.0661T_r + 2.7048T_r^{\,2} - 1.2219T_r^{\,3} \tag{11}$$

The above relation is used in the present work.

In this work, the NDD mixing rules developed by Avlonitis et al.[28] are applied to describe mixing in the a parameter:

$$a = a^C + a^A \tag{12}$$

where a^C is given by the classical quadratic mixing rules as follows:

$$a^C = \sum_i \sum_j x_i x_j a_{ij} \tag{13}$$

and b, c, and a_{ij} parameters are expressed by

$$b = \sum_i x_i b_i \tag{14}$$

$$c = \sum_i x_i c_i \tag{15}$$

$$a_{ij} = (1 - k_{ij})\sqrt{a_i a_j} \tag{16}$$

where k_{ij} is the standard BIP.

The term a^A corrects for asymmetric interaction, which cannot be efficiently accounted for by classical mixing rules:

$$a^A = \sum_p x_p^{\,2} \sum_i x_i a_{pi} l_{pi} \tag{17}$$

$$a_{pi} = \sqrt{a_p a_i} \tag{18}$$

$$l_{pi} = l_{pi}^0 - l_{pi}^1(T - T_0) \tag{19}$$

where p is the index of polar components and l is the BIP for the asymmetric term.

Using the VPT-EoS [27] and the NDD mixing rules,[28] the fugacity of each component in all fluid phases is calculated from

$$\ln \phi_i = \frac{1}{RT}\int_V^{\infty}\left[\left(\frac{\partial P}{\partial n_i}\right)_{T,V,n_{j\neq i}} - RT/V\right] dV - \ln Z \quad \text{for } i = 1, 2, ..., M \tag{20}$$

$$f_i = x_i \phi_i P \tag{21}$$

Table 4. Experimental and Calculated Ethane Mole Fraction in the Aqueous Phase of the Ethane−Water System[a]

T/K	P_{exp}/MPa	$x_{exp} \times 10^3$	AAD(exp)/%	$x_{cal} \times 10^3$	AD/%	T/K	P_{exp}/MPa	$x_{exp} \times 10^3$	AAD(exp)/%	$x_{cal} \times 10^3$	AD/%
274.26	0.393	0.2237	0.3	0.233	4.1	303.21	0.719	0.2396	1.1	0.227	5.1
274.26	0.4922	0.2841	0.5	0.288	1.4	303.21	1.093	0.346	2.7	0.334	3.5
278.06	0.4004	0.205	1.3	0.216	5.2	303.22	1.598	0.4719	1.5	0.464	1.6
278.04	0.6128	0.3106	2.9	0.322	3.7	303.23	2.299	0.6295	1.4	0.622	1.2
278.07	0.8126	0.4143	2.5	0.416	0.5	303.22	2.932	0.7415	2.3	0.741	0.0
283.12	0.473	0.225	3.6	0.225	0.1	303.22	3.977	0.8827	0.6	0.892	1.1
283.1	0.8122	0.3676	1.2	0.371	1.0	313.17	0.439	0.1337	2.1	0.122	8.8
283.1	1.2232	0.53	2.5	0.533	0.5	313.19	0.965	0.2623	0.9	0.258	1.7
288.08	0.4844	0.203	4.7	0.207	1.8	313.19	1.497	0.3841	1.5	0.382	0.5
288.08	1.0426	0.4227	4.3	0.419	1.0	313.19	1.987	0.4799	1.4	0.485	1.1
288.06	2.0801	0.7411	0.7	0.739	0.3	313.19	2.492	0.583	1.6	0.581	0.4
293.33	0.382	0.1464	1.9	0.148	1.3	313.19	3.088	0.6887	2.8	0.679	1.4
293.31	1.01	0.369	3.4	0.368	0.2	313.18	4.669	0.8703	2.6	0.872	0.2
293.3	1.852	0.6073	4.0	0.615	1.3	323.17	0.397	0.0983	1.5	0.096	1.9
293.3	2.963	0.8647	1.2	0.863	0.2	323.19	0.947	0.2231	0.9	0.224	0.4
293.31	3.632	0.9696	0.2	0.970	0.0	323.19	1.989	0.4336	1.6	0.434	0.0
298.3	0.4486	0.1676	0.4	0.158	5.8	323.2	3.03	0.5877	2.1	0.605	2.9
298.37	0.8992	0.2972	0.5	0.303	2.0	323.18	3.963	0.7279	0.9	0.728	0.0
298.35	1.377	0.4498	0.5	0.442	1.7	323.2	4.838	0.8154	1.9	0.818	0.3
298.42	2.021	0.6068	1.5	0.605	0.2	343.08	0.44	0.0854	0.5	0.085	0.1
298.32	2.7539	0.7699	0.3	0.762	1.1	343.06	1.503	0.272	1.9	0.285	4.7
298.31	4.1297	0.9592	2.8	0.964	0.5	343.06	2.895	0.4997	0.4	0.501	0.3
303.19	0.373	0.1341	2.1	0.121	9.5	343.06	4.952	0.7376	0.4	0.738	0.1

[a] AAD: average absolute deviation between samples. $AAD(exp) = (1/N)\sum^N|(\bar{x}_{exp} - x_{exp})/\bar{x}_{exp}|$. AD: absolute deviation. $AD = |(x_{exp} - x_{cal})/x_{exp}|$.

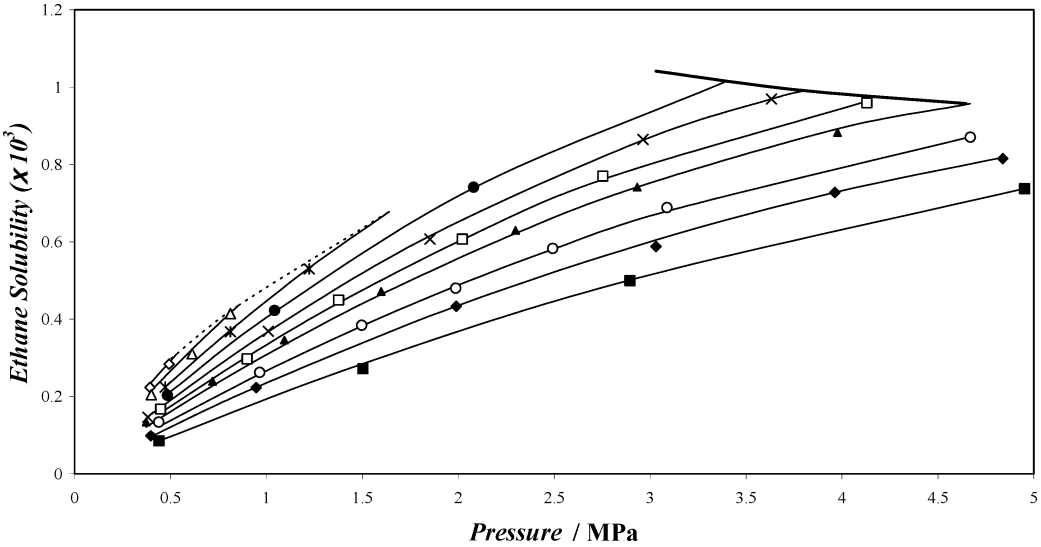

Figure 2. Experimental and calculated ethane solubility (mole fraction) in the aqueous phase as a function of pressure at various temperatures: ◇, 274.26 K; △, 278.06 K; *, 283.11 K; ●, 288.07 K; ×, 293.31 K; □, 298.35 K; ▲, 303.22 K; ○, 313.19 K; ◆, 323.19 K; ■, 343.06 K. Solid curves: calculated with the VPT-EoS[27] and NDD mixing rules[28] with parameters from Table 5. Bold solid curve: ethane vapor pressure. Dashed curve: hydrate phase boundary.[32,33]

where ϕ_i, V, M, n_i, Z, and f_i are the fugacity coefficient of component i in the fluid phases, volume, number of components, number of moles of component i, compressibility factor of the system, and fugacity of component i in the fluid phases, respectively.

4. Results and Discussion

The experimental and calculated gas solubility data are reported in Table 4 and are plotted in Figure 2.

As mentioned earlier, the BIPs between ethane and water are adjusted directly to the measured ethane solubility data through a Simplex algorithm using the objective function, FOB, displayed in eq 22, where N is

$$\mathrm{FOB} = \frac{1}{N}\sum_{1}^{N}\left|\frac{x_{i,\mathrm{exp}} - x_{i,\mathrm{cal}}}{x_{i,\mathrm{exp}}}\right| \qquad (22)$$

Table 5. BIPs between Ethane, hc, and Water, w, for the VPT-EoS[27] and NDD Mixing Rules[28]

system	k_{w-hc}	l^0_{w-hc}	$l^1_{w-hc} \times 10^4$
ethane−water	0.544 21	1.562 94	35.2275

the number of data points, $x_{i,exp}$ is the measured property, and $x_{i,cal}$ is the calculated property. Table 5 reports BIP values adjusted between ethane and water used in this work. It can be noticed that the value of the first BIP, k_{ij}, is of the same order as the BIP of the classical mixing rules without an asymmetric term for a light hydrocarbon−water system.

Our isothermal $P-x$ data sets for the ethane−water system are well represented with the VPT-EoS[27] and NDD mixing rules[28] ($AAD = (1/N)\sum^N|[(x_{experimental} - x_{calculated})]/x_{experimental}| = 1.8\%$). Some ethane solubility data reported in the literature between 293.2 and 303.2 K are plotted in Figure 3 and compared with the new

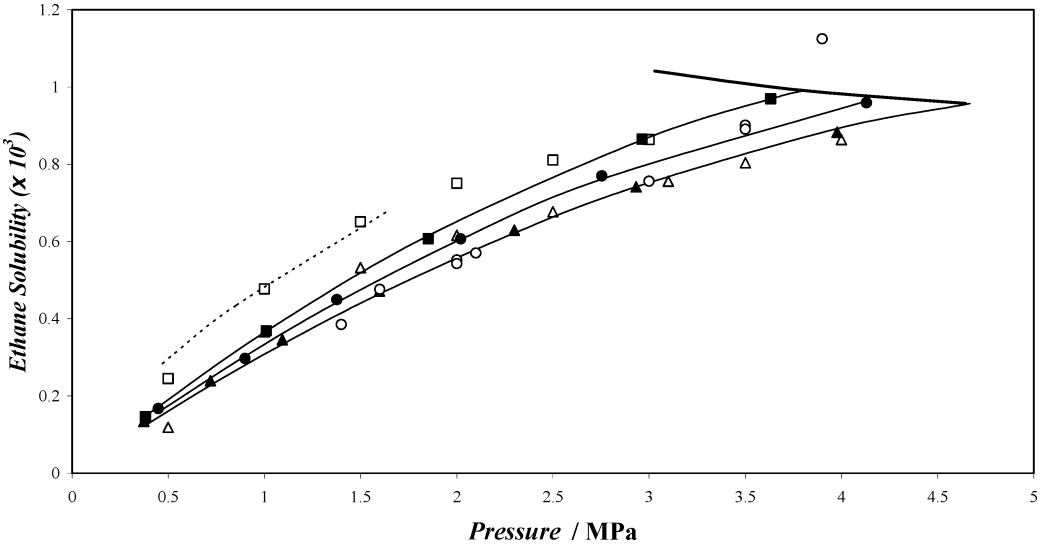

Figure 3. Comparison of experimental ethane solubilities (mole fraction) in water: □, 293.2 K, from Wang et al.;[3] ■, 293.31 K, this work; ○, 298.15 K, from Kim et al.;[4] ●, 298.35 K, this work; △, 303.2 K, from Wang et al.;[3] ▲, 303.22 K, this work. Solid curves: calculated with the VPT-EoS[27] and NDD mixing rules[28] with parameters from Table 5. Bold solid curve: ethane vapor pressure. Dashed curve: hydrate phase boundary.[32,33]

Table 6. Experimental and Predicted Water Mole Fractions in the Vapor Phase of the Ethane−Water System

T/K	*P*/MPa	y_{exp}	y_{prd}	AD/%
		Coan and King[21]		
298.15	2.442	0.001 42	0.001 324	6.76
	2.969	0.001 11	0.001 081	2.61
	3.597	0.000 9	0.000 871	3.22
	3.607	0.000 93	0.000 868	6.67
323.15	2.28	0.005 63	0.005 571	1.05
	2.969	0.004 32	0.004 286	0.79
	2.969	0.004 32	0.004 286	0.79
	2.969	0.004 37	0.004 286	1.92
	3.577	0.003 54	0.003 551	0.31
	3.627	0.003 54	0.003 501	1.10
348.15	2.33	0.017 5	0.017 173	1.87
	2.371	0.016 9	0.016 881	0.11
	3.03	0.013 2	0.013 275	0.57
	3.627	0.010 9	0.011 124	2.06
373.15	2.594	0.041 4	0.041 156	0.59
	2.928	0.036 7	0.036 582	0.32
	2.989	0.036	0.035 856	0.40
	3.638	0.029 6	0.029 63	0.10
		Song and Kobayashi[15]		
288.65	3.421	0.000 525	0.000 497	5.33
294.45	3.876	0.000 65	0.000 616	5.22
299.85	4.345	0.000 716	0.000 729	1.80
303.75	4.714	0.000 736	0.000 792	7.61
		Althaus[12]		
278.15	0.5	0.001 754	0.001 76	0.37
283.15	0.5	0.002 443	0.002 477	1.41
283.15	1.5	0.000 81	0.000 834	2.99
288.15	1.5	0.001 123	0.001 159	3.20
288.15	2	0.000 833	0.000 869	4.38
288.15	2.5	0.000 664	0.000 691	4.11
293.15	1.5	0.001 547	0.001 59	2.75
293.15	2	0.001 193	0.001 194	0.11
293.15	2.5	0.000 917	0.000 952	3.79
293.15	3	0.000 75	0.000 784	4.58
		Mohammadi et al.[1]		
282.93	0.506	0.002 442	0.002 412	1.23
288.11	1.859	0.001 031	0.000 933	9.51
292.95	1.049	0.002 204	0.002 237	1.50
293.1	1.926	0.001 305	0.000 236	5.29
293.1	2.99	0.000 832	0.001 236	5.77

experimental data and the predictions of the model developed in this work. As can be seen, the data reported by Kim et al.[4] are dispersed at different pressure conditions. The data reported by Wang et al.[3] show large deviations, especially at low temperatures and pressures.

To further evaluate the performance of the model, some of the available experimental data on the water content of the vapor phase are compared with the predictions of the model. Table 6 reports a comparison between experimental values and the predictions of the model. The literature ethane−water content data and the predictions of the model show satisfactory agreement, demonstrating the reliability of the techniques and the predictive model used in this work.

5. Conclusions

New experimental data on the solubility of ethane in water were generated over a wide range of temperatures (i.e., 274.26−343.08 K) and pressures of up to 4.952 MPa.

The VPT-EoS[27] with NDD mixing rules[28] was employed to model the phase behavior of the ethane−water system. The new experimental data were employed in tuning of the BIPs between ethane and water.

The model predictions on C_2 solubility in the aqueous phase as well as the water content of the vapor phase in water−ethane systems have been compared with independent experimental data. The results showed good agreement, demonstrating the reliability of the experimental techniques and thermodynamic modeling used in this work.

Acknowledgment

The financial support by the European Infrastructure for Energy Reserve Optimization (EIERO) provided the opportunity for this joint work, which is gratefully acknowledged.

Appendix: Calculation of the Fugacity Coefficient Using an EoS

The following general form can be used for expressing any cubic equation of state:[35]

$$P = \frac{RT}{v-b} - \frac{a}{v^2 + uv - w^2} \qquad \text{(A.1)}$$

The fugacity coefficient for component i in a mixture can be expressed as[35]

$$\ln \phi_i = -\ln(Z - B) + \frac{B_i' B}{Z - B} + \frac{A}{\sqrt{U^2 + 4W^2}}\left[A_i' - \frac{U_i' U^2 + 4W_i' W^2}{U^2 + 4W^2}\right] \ln\left[\frac{2Z + U - \sqrt{U^2 + 4W^2}}{2Z + U + \sqrt{U^2 + 4W^2}}\right] - A\left[\frac{2(2Z + U)W_i' W^2 + (UZ - 2W^2)U_i' U}{(Z^2 + UZ - W^2)(U^2 + 4W^2)}\right] \quad \text{(A.2)}$$

where

$$A = Pa/(RT)^2 \quad \text{(A.3)}$$

$$B = Pb/RT \quad \text{(A.4)}$$

$$U = Pu/RT \quad \text{(A.5)}$$

$$W = Pw/RT \quad \text{(A.6)}$$

$$Z = Pv/RT \quad \text{(A.7)}$$

and

$$A_i' = \frac{1}{na}\left[\frac{\partial(n^2 a)}{\partial n_i}\right]_{T, n_{j \neq i}} \quad \text{(A.8)}$$

$$B_i' = \frac{1}{b}\left[\frac{\partial(nb)}{\partial n_i}\right]_{T, n_{j \neq i}} \quad \text{(A.9)}$$

$$U_i' = \frac{1}{u}\left[\frac{\partial(nu)}{\partial n_i}\right]_{T, n_{j \neq i}} \quad \text{(A.10)}$$

$$W_i' = \frac{1}{w}\left[\frac{\partial(nw)}{\partial n_i}\right]_{T, n_{j \neq i}} \quad \text{(A.11)}$$

The compressibility factor Z is given by the following dimensionless equation:[35]

$$Z^3 - (1 + B - U)Z^2 + (A - BU - U - W^2)Z - (AB - BW^2 - W^2) = 0 \quad \text{(A.12)}$$

List of Symbols

AAD = average absolute deviation
AD = absolute deviation = $|(x_{exp} - x_{cal\ or\ prd})/x_{exp}|$
BIP = binary interaction parameter
EoS = equation of state
NDD = non-density-dependent mixing rules
VPT-EoS = Valderrama modification of the Patel−Teja equation of state
F = parameter of the equation of state
M = number of components
N = number of experimental points
P = pressure [Pa]
R = universal gas constant [J/(mol K)]
T = temperature [K]
V = volume [m^3]
Z = compressibility factor
a = attractive parameter of the equation of state [Pa m^6/mol^2]
$\bar{a}$ = parameter of the equation of state [Pa m^6/mol^2]
b = parameter of the equation of state [m^3/mol]
c = parameter of the equation of state [m^3/mol]
f = fugacity
k = binary interaction parameter for the classical mixing rules
l = constant for the binary interaction parameter for the asymmetric term
n = number of moles
u = parameter of the equation of state in general form
v = molar volume [m^3/mol]
w = parameter of the equation of state in general form
x = liquid mole fraction
y = vapor mole fraction

Greek Symbols

Ψ = power parameter in the VPT-EoS
Ω = parameter in the VPT-EoS
α = temperature-dependent function
ϕ = fugacity coefficient
ω = acentric factor

Superscripts

A = asymmetric properties
C = classical properties
0 = non-temperature-dependent term in NDD mixing rules
1 = temperature-dependent term in NDD mixing rules

Subscripts

cal = calculated property
exp = experimental property
hc = hydrocarbon
min = minimum
max = maximum
prd = predicted property
a = index for properties
b = index for properties
c = critical property
c_* = index for properties
i, j = molecular species
p = polar compound
r = reduced properties
w = water
0 = reference property

Literature Cited

(1) Mohammadi, A. H.; Chapoy, A.; Richon, D.; Tohidi, B. Experimental Measurement and Thermodynamic Modeling of Water Content in Methane and Ethane Systems. *Ind. Eng. Chem. Res.* **2004**, in press.

(2) Mohammadi, A. H.; Chapoy, A.; Tohidi, B.; Richon, D. A Semi-Empirical Approach for Estimating Water Content of Dry and Sweet Natural Gases. *Ind. Eng. Chem. Res.* **2004**, in press.

(3) Wang, L.-K.; Chen, G.-J.; Han, G.-H.; Guo, X.-Q.; Guo, T.-M. Experimental study on the solubility of natural gas components in water with or without hydrate inhibitor. *Fluid Phase Equilib.* **2003**, *207*, 143−154.

(4) Kim, Y. S.; Ryu, S. K.; Yang, S. O.; Lee, C. S. Liquid Water−Hydrate Equilibrium Measurements and Unified Predictions of Hydrate-Containing Phase Equilibria for Methane, Ethane, Propane and Their Mixtures. *Ind. Eng. Chem. Res.* **2003**, *42*, 2409−2414.

(5) Reichl, A. Dissertation, Technische Universität Berlin, 1996 (data from Dortmund Data Base).

(6) Danneil, A.; Tödheide, K.; Franck, E. U. Verdampfungsleichgewichte und kritische Kurven in den Systemen Äthan/Wasser und *n*-Butan/Wasser bei hohen Drücken. *Chem. Ing. Tech.* **1967**, *13*, 816−821 (quoted in *Ethane*; IUPAC Solubility Data Series 9; Pergamon Press: New York, 1982).

(7) Anthony, R. G.; McKetta, J. J. Phase Equilibrium in the Ethylene−Water System. *J. Chem. Eng. Data* **1967**, *12* (1), Jan, 17−20.

(8) Czerski, L.; Czaplinski, A. *Ann. Soc. Chim. Polonorum* **1962**, *36*, 1827−1834 (Poland; quoted in *Ethane*; IUPAC Solubility Data Series 9; Pergamon Press: New York, 1982).

(9) Culberson, O. L.; McKetta, J. J. Phase Equilibria in Hydrocarbon−Water Systems II, The Solubility of Ethane in Water at Pressures to 10000 psi. *Petr. Trans. AIME* **1950**, *189*, 319−322.

(10) Culberson, O. L.; Horn, A. B.; McKetta, J. J. Phase Equilibria in Hydrocarbon−Water Systems: The Solubility of Ethane in Water at Pressures up to 1200 Pounds per Square Inch. *Petr. Trans. AIME* **1950**, *189*, 1−6.

(11) Chapoy, A.; Coquelet, C.; Richon, D. Measurement of the Water Solubility in the Gas Phase of the Ethane + Water Binary System near Hydrate Forming Conditions. *J. Chem. Eng. Data* **2003**, *48*, 957−966.

(12) Althaus, K. *Fortschr.−Berichte VDI* **1999**, *3*, 350 (in German). Oellrich, L. R.; Althaus, K. GERG−Water Correlation (GERG Technical Monograph TM14) Relationship Between Water Content and Water Dew Point Keeping in Consideration the Gas Composition in the Field of Natural Gas. *Fortschr.−Berichte VDI* **2000**, *3* (No. 679) (in English).

(13) Song, K. Y.; Kobayashi, R. The water content of ethane, propane and their mixtures in equilibrium with liquid water or hydrates. *Fluid Phase Equilib.* **1994**, *95*, 281−298.

(14) Namiot, A. Yu. *Rastvorimost' gazov v vode. Spravochnoe posobie* (*Solubility of Gases in Water: A Handbook*); Nedra: Moscow, 1991 [quoted in Ugrozov, V. V. Equilibrium Compositions of Vapor−Gas Mixtures over Solutions. *Zh. Fiz. Khim*. **1996**, *70* (7), 1328−1329 (in Russian)].

(15) Song, K. Y.; Kobayashi, R. *Water Content of Ethane, Propane, and Their Mixtures in Equilibrium with Liquid Water or Hydrates*; GPA Research Report 132; GPA: Tulsa, OK, Dec 1991.

(16) Sloan, E. D.; Sparks, K. A.; Johnson, J. J. Two-Phase Liquid Hydrocarbon−Hydrate Equilibrium for Ethane and Propane. *Ind. Eng. Chem. Res*. **1987**, *26*, 1173−1179.

(17) Bourrie, M. S.; Sloan, E. D. *Water Content of NGL in Presence of Hydrates*; GPA Research Report 100; GPA: Tulsa, OK, June 1986.

(18) Sparks, K. A.; Sloan, E. D. *Water Content of NGL in Presence of Hydrates*; GPA Research Report 71; GPA: Tulsa, OK, Sept 1983.

(19) Parrish, W. R.; Pollin, A. G.; Schmidt, T. W. Properties of Ethane-Propane Mixes, Water Solubility and Liquid Densities. *Proceedings of the 61st Annual Convention of the Gas Processes Association*, Dallas, TX, 1982; pp 164−170.

(20) Pollin et al. Internal Report, Phillips Petroleum Co., 1982 (quoted in ref 18).

(21) Coan, C. R.; King, A. D. Solubility of Water in Compressed Carbon Dioxide, Nitrous Oxide and Ethane. Evidence for Hydration of Carbon Dioxide and Nitrous Oxide in the Gas Phase. *J. Am. Chem. Soc*. **1971**, *93*, 1857−1862.

(22) Anthony, R. G.; McKetta, J. J. Phase Equilibrium in the Ethylene−Ethane−Water System *J. Chem. Eng. Data* **1967**, *12* (1), Jan, 21−28.

(23) Reamer, H. H.; Olds, R. H.; Sage, B. H.; Lacey, W. N. Phase Equilibria in Hydrocarbon Systems. Composition of Dew-Point Gas in Ethane−Water System. *Ind. Eng. Chem*. **1943**, *35* (7), July, 790−793.

(24) Chapoy, A.; Coquelet, C.; Richon, D. Solubility measurement and modeling of water in the gas phase of the methane/water binary system at temperatures from 283.08 to 318.12 K and pressures up to 34.5 MPa. *Fluid Phase Equilib.* **2003**, *214*, 101−117.

(25) Chapoy, A.; Mohammadi, A. H.; Richon, D.; Tohidi, B. Gas Solubility Measurement and Modeling for Methane−Water and Methane−Ethane−*n*-Butane−Water Systems at Low-temperature Conditions. *Fluid Phase Equilib.* **2004**, *220*, 113−121.

(26) Chapoy, A.; Mohammadi, A. H.; Tohidi, B.; Richon, D. Gas Solubility Measurement and Modeling for Nitrogen−Water System from 274.18 K up to 363.02 K. *J. Chem. Eng. Data* **2004**, in press.

(27) Valderrama, J. O. A generalized Patel−Teja equation of state for polar and non-polar fluids and their mixtures. *J. Chem. Eng. Jpn.* **1990**, *23*, 87−91.

(28) Avlonitis, D.; Danesh, A.; Todd, A. C. Prediction of VL and VLL equilibria of mixtures containing petroleum reservoir fluids and methanol with a cubic EoS. *Fluid Phase Equilib.* **1994**, *94*, 181−216.

(29) Laugier, S.; Richon, D. New Apparatus to Perform Fast Determinations of Mixture Vapor−Liquid Equilibria up to 10 MPa and 423 K. *Rev. Sci. Instrum*. **1986**, *57*, 469−472.

(30) Guilbot, P.; Valtz, A.; Legendre, H.; Richon, D. Rapid On-Line Sampler Injector. *Analusis* **2000**, *28*, 426−431.

(31) Avlonitis, D. A. Multiphase Equilibria in Oil−Water Hydrate Forming Systems. M.Sc. Thesis, Heriot-Watt University, Edinburgh, Scotland, 1988.

(32) Avlonitis, D. A. Thermodynamics of Gas Hydrate Equilibria. Ph.D. Thesis, Heriot-Watt University, Edinburgh, Scotland, 1992.

(33) Tohidi, B.; Burgass, R. W.; Danesh, A.; Todd, A. C. Hydrate inhibition effect of produced water, Part 1. Ethane and propane simple gas hydrates. *SPE 26701, Proceedings of the SPE Offshore Europe 93 Conference*, 1993; pp 255−264.

(34) Tohidi-Kalorazi, B. Gas Hydrate Equilibria in the Presence of Electrolyte Solutions. Ph.D. Thesis, Heriot-Watt University, Edinburgh, Scotland, 1995.

(35) Danesh, A. *PVT and Phase Behaviour of Petroleum Reservoir Fluids*, 1st ed.; Elsevier: Amsterdam, The Netherlands, 1998.

Received for review March 31, 2004
Revised manuscript received May 17, 2004
Accepted May 25, 2004

IE049747E